ANALYSIS OF DIRECT FUNCTIONALIZATION OF NANOSILICA WITH APTES FOR APPLICATION IN CEMENTITIOUS COMPOSITES

Kleymer Henrique Pereira Silva[1], Maria José De Souza Serafim[2], Andreia de Paula[3] Yuri Sotero Bomfim Fraga[4] and João Henrique da Silva Rego[5]

[1] University of Brasília - UnB, 70910-900, Brasília, DF.
kleymerhenriquepereirasilva@gmail.com
[2] University of Brasília - UnB, 70910-900, Brasília, DF.
mariajss19@yahoo.com.br
[3] University of Brasília - UnB, 70910-900, Brasília, DF.
paula_adp@yahoo.com.br
[4] Federal University of Acre – UFAC, 69920-900, Rio Branco, AC.
yurisotero.engcivil@gmail.com
[5] University of Brasília - UnB, 70910-900, Brasília, DF.
jhenriquerego@unb.br

ABSTRACT

This article has the objective of discussing the effects of direct functionalization of NS) with aminosilane from a colloidal NS and reagent 3 -aminopropyltriethoxysilane (APTES), without using any chemical solvent. A first reaction was prepared with the reagents 4 mL of APTES, 100 mL of dichloromethane (H2CCl2) and 60 mL, forming NSF4. An alternative reaction process was developed, removing dichloromethane and without using any other solvent, forming NSF4WD. Some techniques were used to evaluate the efficiency of the reactions: pH, solids content, DLS, Zeta potential, XRD, TGA and FTIR. Portland cement pastes and mortars were produced to evaluate the effect of NS produced by the two different functionalization processes on hydration kinetics, porosity and compressive strength (at 1, 3, 7 and 28 days). The results showed that the use of dichloromethane in the functionalization process does not present significant contributions, since NSF4WD presented similar results to NSF4. It is concluded that the direct alternative method proved to be effective in grafting APTES onto the NS surface, in addition to meet the principles of Green Chemistry by not using toxic solvents, minimizing negative impacts on the environment and optimizing the functionalization process.

KEYWORDS: *Direct functionalization; Dichloromethane; Green Chemistry; Nanosilica, Portland cement.*

I. INTRODUCTION

Nanosilica (NS) is classified as a pozzolanic material with particles of structural order equal to or less than 100 nm, and can be considered a Supplementary Cementitious Material (SCM) with high reactivity [1, 2, 6,]. NS is a highly efficient SCM for modifying cementitious products, even when used in small concentrations (<3%) [2, 3].

Experimental evidences that indicate changes in the microstructure, which effectively contribute to modifying the physical-chemical properties of the materials, prove the impact of incorporating NS into cementitious composites. It is known that NS provides an improvement in the resistance measurements of Portland cement pastes, especially in the initial ages (up to 3 days), by combining its high surface area with a more efficient pozzolanic reaction, producing a denser and greater microstructure durability [1-4, 6, 7, 9,12, 13, 19, 21, 30-34, 38, 44, 47, 48]. On the other hand, the high surface energy of the NS particle generates a high agglomeration potential, which can cause damage to the properties of the

material in its fresh (rheology and workability) and hardened (mechanical properties) state. Compression resistance may be compromised due to acceleration of initial hydration reactions promoted by NS, which can form a layer of C-S-H on the clinker surface, impairing hydration at more advanced ages [2,5,31,36].

A major focus in recent research is the study of procedures capable of mitigating these negative effects, such as the incorporation of new functional groups on the surface of the NS, a procedure called functionalization [5-10]. The functionalization of NS, or silanization, consists on chemical alteration of its surface by replacing the silanol groups (OH) with the grafting of new chemical functions of greater interest, e.g. amino silane groups.

In the literature, some research has investigated the effect of applying nanosilica functionalized with aminosilane (NSF) in cementitious materials [2,6,7,10-13,31-33,38,43,45,47]. It is observed that NSF caused a delay in the hydration of these composites, reducing the initial precipitation rate of the hydrates and the compressive strength of the pastes at the initial ages. However, after 7 days of hydration, NSF makes the microstructure of the composite denser and, by doing this, provides increases in the mechanical properties and durability of cement-based composites, due to the synergy between the pozzolanic effects.

Over the last few years, the NS functionalization process has undergone several changes aimed at minimizing the number of products involved in the process and reducing the number of steps in product preparation. At the first moment, the process was made by using a solution composed of dichloromethane (H2CCl2), ammonium hydroxide (NH4OH) and APTES added together with NS in a round-bottom flask coupled to a condenser to avoid loss of reagents by evaporation, at room temperature [6]. Further researches aimed to make this process technologically and ecologically more efficient, simplifying the steps and materials used in the functionalizing solution [2,11]. The big leap in optimizing the NSF synthesis process came with the exclusion of ammonium hydroxide from the mixture, thus using only dichloromethane as a solvent in the solution [7,10-13].

Despite the evolution of NS functionalization with APTES, dichloromethane is still used as a chemical reagent in this process. The H2CCl2 is a colorless, non-flammable and very volatile liquid. When inhaled, dichloromethane is capable of causing headache, nausea, memory loss and dizziness, in addition to being considered a possible carcinogenic material by the International Agency for Research on Cancer (IARC) [14]. The continued application of this product in the field of materials technology goes against the concepts of Green Chemistry, a branch of classical Chemistry, whose conceptualization began to be discussed in the 90s by John Warner and Paul Anastas, members of the North American environmental agency (EPA). Its application focuses on the development of chemical products and processes that seek to reduce or eliminate the use and generation of substances that are dangerous to the environment and human health, such as dichloromethane.

The objective of this study is to verify the effect of functionalized nanosilica directly on the hydration kinetics and on the physical and mechanical properties of cementitious materials when compared with conventional functionalized nanosilica, producing an environmentally friendly alternative method, without the use of any solvent, in order to meet the principles of Green Chemistry. In Section 2 of this article, the methodology and materials used are presented, as well as the tests to characterize both the nanosilicas (NS's) and the cementitious compounds developed with their addition. In section 3, the results are exposed and discussed. Finally, section 4 concludes the analyzes developed regarding the efficiency of the aminofunctionalization of the processes used.

II. EXPERIMENTAL DETAILS

2.1. Materials

For the functionalization process, NS in colloidal suspension with a content of 30% was used - LEVASIL CB30 from NOURYON Chemicals, 3-Aminopropyltriethoxysilane (APTES) reagent with 99% purity from SIGMA-ALDRICH, dichloromethane PA 99.8% and deionized water. The production of cementitious materials consisted of using Portland CPV-ARI cement (with a low level of additions and specific surface area 4692 cm 2 /g, meeting the Brazilian standard [26]), equivalent to type III

ASTM C150 and CEM IEN 197, and superplasticizing additive (SP) based on aqueous polycarboxylate solution. Table 1 presents the chemical compositions referring to NS and the cement used in this study.

Table 1. Chemical composition of CP V-ARI and NS

Name	Chemical composition (%)										
	SiO_2	Al_20_3	Fe_2O_3	CaO	K_2O	TiO_2	MnO	SO_3	LOI	Specific mass (g/cm^3)	Average particle size
CP	23.7	7.2	3.2	52.4	1.0	0.4	0.1	5.8	5.7	3.06	16.4 (μm)
NS	92	-	-	0.08	0.02	-	-	-	8	1.20	8.3 (nm)

2.2. Functionalization and Characterization of Nanosilica

Two NSF functionalization processes with APTES were developed. In both cases, the APTES/NS ratio of 4 mL/60 mL was adopted, which presented more satisfactory results in the literature [2,7,13]. Initially, functionalization was carried out in the traditional way, a method already developed by other authors [7, 10-13]. The solution of NS, APTES and 100 mL dichloromethane was prepared in a round-bottom flask sealed with the coupling of a condenser, to avoid possible loss of reagents through evaporation. The system was subjected to constant agitation on a magnetic stirrer at 1500 rpm for 24 hours, forming NSF4. After the end of the stirring time, the mixture was transferred to a separation funnel to separate the dichloromethane from the phase containing NSF4, subsequently transferred to a beaker and mixed with 100 mL of deionized water. The final stage consists on ultrasonication of NSF4 to delay the non-agglomeration of particles through the ultrasonic processor with an amplitude of 65%, at room temperature for 10 minutes, and every 50s the equipment rests for 10s [13,18].

A second form of functionalization consists on using an alternative process in which the NS functionalization reaction is direct with APTES, without the addition of chemical solvent, giving rise to NSF4WD. The process occurs in a similar way to the traditional one, but without the addition of dichloromethane and without the need of separating the chemical solvent at the end of the reaction period. Therefore, this methodology meets the principles of Green Chemistry, so debated in the modern scenario, which are based on the idea that chemical processes that generate environmental problems can be replaced by less polluting or non-polluting alternatives, reducing toxicity and waste of this activity minimizing the number of products and steps required. A synthesis of both described processes can be seen in Figure. 1.

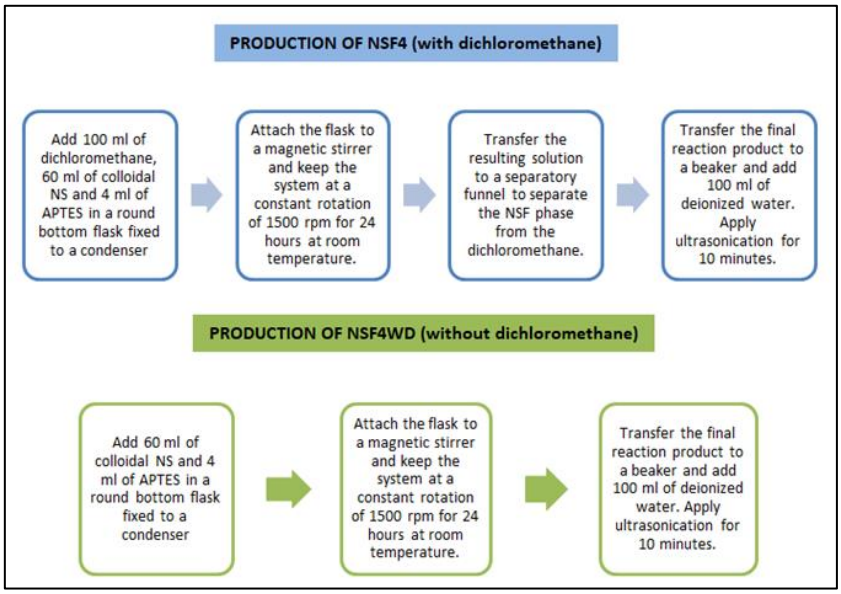

Figure 1. Synthesis of NS functionalization processes (with and without dichloromethane)

Physical and microstructural analyzes were used to characterize the samples for the purpose of evaluating the functionalization efficiency, determined by the level of APTES coupling on the NS surface, comparing the use of NSF4 with NSF4WD. The solid content test and pH measurement were realized with the purpose of obtaining the volume of liquid, which must be subtracted from the water used in the paste and mortar mixing process, and the alkalinity of the materials, respectively. Table 2 shows the results of these tests.

Table 2. Solid content and pH values of nanosilicas

Sample	Suspension coloring	Solid content	pH
NS	Whitish	32.5	10.7
NSF4	Whitish	15.3	11.2
NSF4WD	Whitish	14.5	11.3

Dynamic Light Scattering (DLS) and Zeta Potential were performed using the Zetasizer Nano ZS90 equipment, with samples dispersed in an aqueous solution. The Zetasizer system determines the particles size by first measuring the Brownian movement of particles in a sample using DLS and then interpreting a size from established theories. To realize the assay, the colloidal NS and NSF samples were inserted into PC51115 and DTS1060C cells.

The X-ray Diffraction analysis was developed in a RIGAKU Última IV model diffractometer according to the parameters of 2 theta: 2 to 60°, step: 0.05°, speed: 5°/min. The TGA was made with the help of SHIMADZU thermal analysis equipment, model DTG-60H, at a heating rate of 10 °C/min up to a temperature of 1000°C, using porcelain crucibles. The FTIR analysis was carried out on a PERKIN ELMER FT-IR Spectrum 400 equipment, in the region between 4000 and 500 cm-1, with KBr tablets in the proportion 2/200 mg. To carry out the tests discussed above, the sample must be in a solid state, therefore, it was necessary to dry the samples, outdoors in a cool and ventilated place, and pulverize them in the porcelain mortar, with the help of a pistil until it results in a fine powder.

2.3. Composition and Characterization of cement pastes and mortars

Table 3 presents the composition of the pastes and mortars produced for the development of this study. The standard replacement content was determined at 1% of NS, NSF4 and NSF4D in relation to the mass of cement used in the reference paste, a value determined in accordance with previous studies [13]. The SP additive was incorporated in a particular quantity into each mixture to obtain the pre-fixed consistency of 110±10mm for the pastes [25], the same levels were applied to the mortars. All pastes were produced with a fixed water/binder ratio = 0.35. The amount of water present in the nanosilicas and superplasticizer additive was subtracted from the total amount to be used in the mixtures. The materials mixing process followed literature recommendations [13, 28].

Table 3. Nomenclature and composition of Portland cement pastes

Material	Abbreviation	Cement (g)	Water (g)	Sand (x4)	NS (g)	NSF4(g)	NSF4WD(g)	SP (%)
Paste	P-REF	2000	691.30	-	-	-	-	0.6
	P-NS	1980	643.96	-	61.54	-	-	1
	P-NSF4	1980	569.09	-	-	137.93	-	0.9
	P-NSF4WD	1980	576.23	-	-	-	130.72	0.9
Mortar	M-REF	700	241.90	335	-	-	-	0.6
	M-NS	693	207.35	335	48.27	-	-	1
	M-NSF4	693	199.14	335	-	48.27	-	0.9
	M-NSF4WD	693	201.70	335	-	-	45.75	0.9

The pastes were investigated regarding the heat of hydration and their porosity, while the mortars were investigated regarding their compressive strength. Isothermal conduction calorimetry was performed

with TAM Ai's Thermometric AB equipment and used to monitor and quantify the heat flow in a 10g sample of each paste in the first 72 hours of hydration, at a temperature of 23°C.

To verify the mechanical properties of the cement mortars produced, the compressive strength test was carried out on 4 cylindrical samples (50x100mm) for each age (1, 3, 7 and 28 days of hydration). To apply the load until disruption, a Denison press model TIA/MC with a maximum capacity of 200 tons was used. The resistance was defined according to recommendations [27], obtaining the average of the individual resistances of the 4 specimens of the same age. ANOVA analysis of variance was performed to verify if there was a significant difference in the compressive strength of the mortars after all ages of hydration. Subsequently, the Duncan test was carried out to join the pastes and mortars into homogeneous and heterogeneous classes of compressive strength.

Mercury intrusion porosimetry (MIP) using Micromeritics Poresizer 9320 was used to evaluate the distribution of pore sizes and the total porosity of the cement pastes produced. The pressure range used in the test was approximately 0.6582 psi to 25.4162 psi and the parameters used were: surface tension of 0.485 N/m, density of 13.5335 g/mL and contact angle of 130°.

III. RESULTS AND DISCUSSIONS

3.1. Characterization of NS's

In this section, the results of the microstructural techniques used for the characterization of both the pure NS and the reactions obtained in the traditional (NSF4) and alternative functionalization processes without dichloromethane (NSF4WD) are presented and discussed, in order to evaluate the efficiency of the procedures used.

3.1.1. XDR

X-ray Diffraction analysis was developed with the aim of determining the degree of crystallinity or amorphism of materials. The XRD spectra of the samples are presented in Figure 2. Note that the samples presented an amorphous halo with relatively low crystallinity and presenting two characteristic broad bands, at 2θ = 10º and 2θ = 23º.

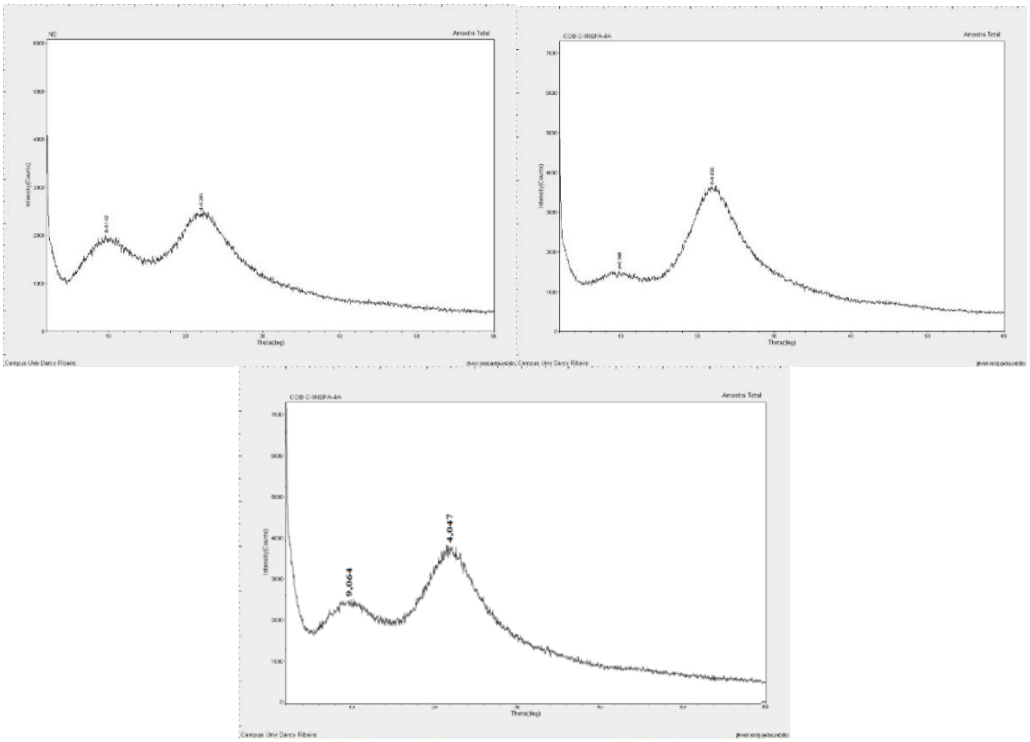

Figure 2. Diffractograms of NS, NSF4 and NSF4WD

Even with the characteristic profile of amorphous silica, it is possible to observe changes in the intensity of the bands in the diffractograms of NSF4 and NSF4WD, suggesting that functionalization interferes with the intensity of the material's peak. In the band centered at 10°, a smoothing of the peak can be seen for functionalized materials, with greater intensity in NSF4. Opposite behavior occurs in the band centered at 23° where a more representative change occurred, now related to the increase in the intensity of the characteristic peaks, mainly for NSF4. The greater change in diffractions, especially at angle 2 θ = 23º, may indicate a greater amount of APTES in the silica network [12].

The results indicated that the silanization of NS mainly affects the crystallographic plane with reflection 2 θ = 23º, a diffraction characteristic of amorphous silica SiO2. Greater variations in vibrations presented by NSF4 may represent greater development of the APTES coating network on NS, indicating greater thickness of the coating layer on the nanoparticles or greater polymerization of these bonds [12]. In general, the diffractograms indicate a characteristically amorphous nature in the nanosilicas, without significant modifications in the displacements of the reflections and in the interplanar planes, highlighting the efficiency and similar behavior between the functionalizations, with emphasis on the alternative process that made it possible to maintain an amorphous character closer to the pure system.

3.1.2. Hydrodynamic diameter, Zeta Potential and TGA

Dynamic Light Scattering (DLS) is a technique frequently used to verify whether an increase in particle size has occurred due to the connection of functional groups on the surface of the NS by determining the medium hydrodynamic diameter of the nanoparticles [8,9,21-24], verifying this variation according to the type and content of functionalization used. The analysis developed in this technique allowed the division of particles into 3 distinct diameter ranges: peak 1 refers to NS in its size close to natural (around 8 nm); peak 2 covers sizes between 49 - 180 nm and the last range covers average diameters bigger than 2000 nm. The results of the hydrodynamic radius and Zeta potential of the samples are shown in Table 4.

Table 4. Result of the hydrodynamic radius, Zeta Potential and TGA of the samples

Sample	Peak 1 (r,nm)	Area 1 (%)	Peak 2 (r,nm)	Area 2 (%)	Peak 3 (r,nm)	Area 3 (%)	Zeta Potential	TGA (300°C - 800°C)
NS	8.3	75.2	49.0	23.6	2196	1.2	-32.3	1.8
NSF4	11.7	80.7	180.0	18.1	2086	1.2	-20.0	5.1
NSF4WD	9.0	57.9	74.1	36.9	2152	5.2	-23.8	4.9

The results show that the alternative functionalization without dichloromethane provided similar results to NSF4 produced by the traditional process, increasing the size of particles functionalized with aminosilane in relation to the size of NS in ranges 1 and 2, behavior expected and described in the literature [7,8, 13]. In peak 1, NSF4WD and NSF4 presented diameters 9% and 41% greater than NS, respectively. This increase indicates the success of the functionalization processes, since it is expected that with the insertion of an additional material on the surface of the NS, an increase in its hydrodynamic radius will occur. NSF4 was the sample that presented both the largest diameter and largest area of particles in this peak, suggesting that dichloromethane intensifies the coupling of aminosilane to NS.

In peak 2, NSF4 also showed a more significant increase in average size than NSF4WD, however covering a relatively smaller percentage of the sample area. The third range is compost of particles with an average size greater than 2,000 nm, being the largest value related to the NSF4WD sample. Peaks 2 and 3 are quite representative because they may be related to a tendency for particles to agglomerate. In these ranges, the alternative functionalization encompassed a larger area of particles (42.10%) than the traditional process (19.30%). This effect may have occurred due to the lower amount of solvent in the NSF4WD reaction medium related to the non-use of dichloromethane.

The efficiency of the alternative functionalization method can be corroborated with the Zeta Potential values, which is associated with the stability of the colloidal suspension. According to the literature, colloidal suspensions that have a Zeta potential close to 30 mV, positive or negative, have high colloidal stability. NSF4 presented a lower Zeta potential than that attributed to NSF4WD (-20 and -23.8,

respectively), having less stability. These results may refer to the APTES content coupled in the functionalized materials. It is known that NS has a negative surface charge due to the presence of silanol groups (OH) on its surface. With functionalization, covalent bonds are built between the APTES molecules and the hydroxylated surface, neutralizing the OH groups on the surface. With this said, the surface charge tends to increase its positive value the higher the content of the functionalizing present agent in the NS [7,13, 37].

The TGA, in turn, made it possible to evaluate the functionalization of the samples based on the variation in the mass loss of the material as a function of the increase in temperature at a programmed rate, comparing them with the NS reference [2,31,32]. Table 4 presents the mass loss values between 300°C and 800°C. The mass loss in this range corresponds to the decomposition of the amine groups, resulting in the separation of the coupling agent from the NSF surface, which can be a parameter used to verify the APTES grafting rate or the efficiency of the material's functionalization [9,33] . The mass loss in the functionalized samples was higher than that of pure NS. This result shows that the functionalization processes were efficient, corroborating the DLS and Zeta Potential results. Furthermore, NSF4 obtained a slightly higher loss value than NSF4WD (4%), which may be an indicator of the greater presence of the coupling agent in traditional functionalization. This behavior may be related to the reaction medium used, since the presence of the solvent increases the dilution of the reaction medium and may promote the adsorption of the aminosilane on the surface of the NS.

It is known that the adsorption process is complex, but it can be simplified into three stages: (I) APTES adsorption begins and increases rapidly over time, since the number of binding sites is sufficiently large. (II) The adsorption rate is reduced due to the gradual reduction of active sites that can be occupied, until adsorption reaches equilibrium. (III) After equilibrium, the remaining content of the functionalizing compound generates a certain degree of saturation in the medium [48]. Therefore, the greater presence of APTES alone does not guarantee greater functionalization efficiency.

3.1.3. Fourier Transform Infrared Spectroscopy (FTIR)

Figure 3 presents the FTIR spectra of the NS's samples and the isolated APTES in the scanning range from 500 to 4000 cm-1 . FTIR makes it possible to identify the bands related to the insertion of APTES on the surface of the functionalized nanosilica, relating a lower transmittance to the greater presence of the material in the functionalization. It is possible to notice the appearance of two bands in the region between 2800 and 3000 cm-1 in NSF4 and NSF4WD, which indicate that functionalization has occurred on the surface of the NS, since they are characteristics of APTES and do not appear in the spectrum of NS. Researches afirm that these bands are associated with the C–H stretching of APTES [31-33], suggesting the presence of aminosilane on the surface of NSF.

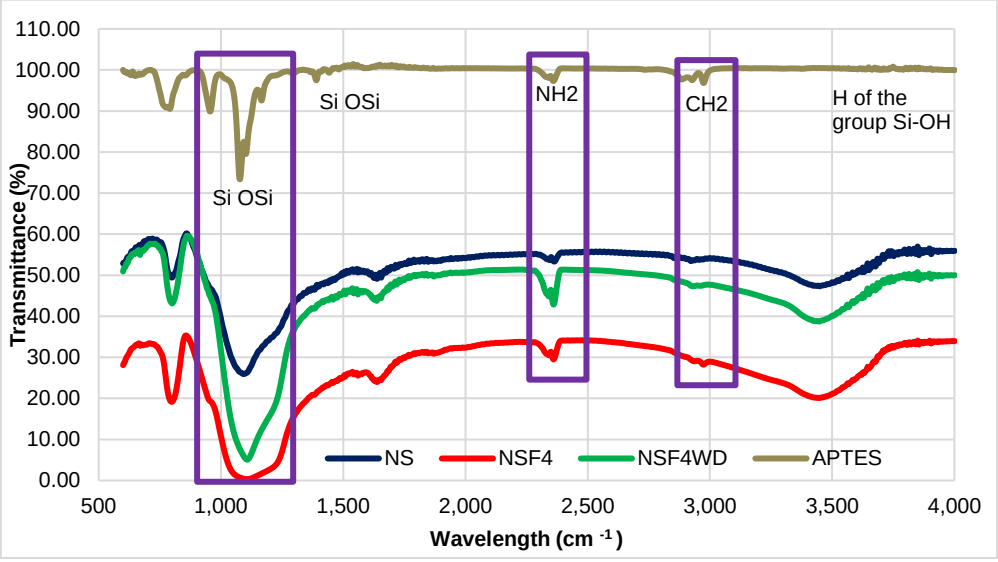

Figure 3. FTIR spectra of NS, NSF4 and NSF4WD

NSF4 and NSF4WD showed the same FTIR spectrometer pattern. It is possible to observe two other ranges that could be observation points for the presence of amine groups: between 1000 cm-1 and 1300 cm-1 and 2300 cm -1 to 2500 cm -1 . The band in the wavelength region from 1000 cm-1 to 1300 cm-1 refers to the Si-O-Si stretching vibration, related to the formation of bonds between the surface of the NS and the APTES. The deepening and widening of the area under these NSF peaks is evident when compared to pure NS, indicating an increase in the concentration of the Si–O–Si bonding system after functionalization. The intensity of the spectrum at this wavelength may indicate that the degree of polymerization of the Si-O tetrahedron increased with functionalization, a condition that confirms that APTES is connected to the surface. The band in the region from 2300 cm-1 to 2500 cm-1 refers to the movement of the NH. According to the literature, APTES forms a covalent bond with silica particles through the OH group and its surface becomes NH-terminated [50].

These results corroborate some researches [37,39,40] which afirm that efficient functionalization produces an increase in siloxane bonding and can decrease transmittance , since the functional groups absorb IR spectra corresponding to the energy of their vibrational signature.

3.2. Characterization of pastes and mortars

In this section, the results of the tests used to characterize the pastes and mortars developed in this research are presented and discussed. Isothermal conduction calorimetry tests, compressive resistance and mercury intrusion porosimetry were used to evaluate the efficiency of the NS, NSF4 and NSF4WD produced on the properties of the mentioned materials.

3.2.1. Hydration Kinetics

The curve produced from the results of the paste isothermal calorimetry test is presented in Figure 4, allowing the evaluation of the effect of different functionalization processes on the cement hydration kinetics. It can be seen that the addition of NS, NSF4 and NSF4WD did not promote the addition of new peaks, but brought significant changes in the intensity and time of the process.

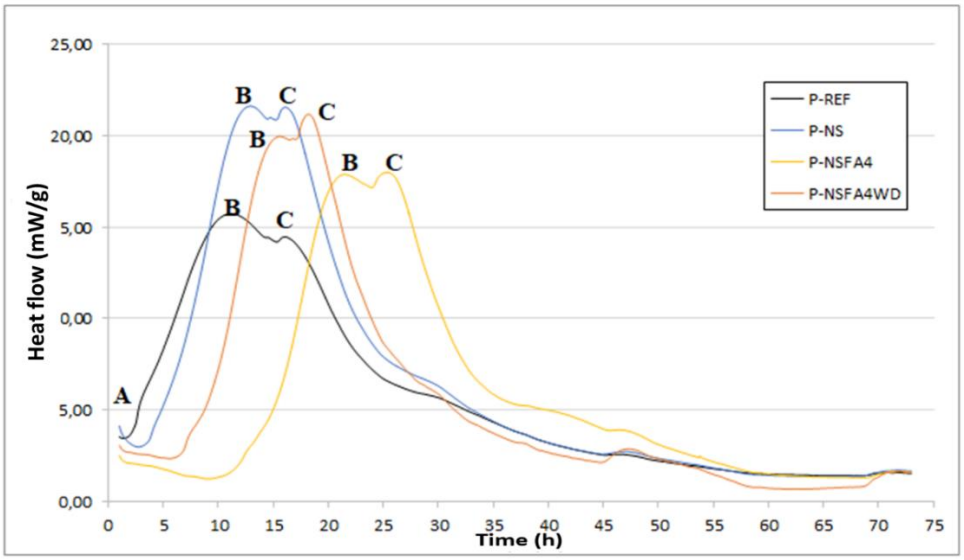

Figure 4. Heat flow released from pastes

NS provided the highest heat flow intensity for the paste (approximately 22 mW/g), while the reference paste presented the lowest heat flow intensity compared with all the other samples (approximately 16 mW/g). The increase in the heat release rate is related to the acceleration of cement hydration caused by the incorporation of small NS particles and the consequent increase in the surface area available in the sample, which facilitates the absorption of calcium ions, increasing the clinker dissolution rate. With the grafting of amine groups onto the NS by functionalization creates a layer of ions on the particles that are released into solution and adsorb to the nucleation sites, hindering the progressive formation of

hydrates [31-33]. This effect is exemplified by the behavior of pastes P-NSF4 and P-NSF4WD, which not only presented a lower heat release rate than NS but also a significant increase in the dormancy period, represented by the initial prolongation of the hydration curve in Figure 5. Sample P-NSF4, with the longest delay, started releasing heat after 12 hours. This time is approximately 10 hours longer than P-REF, 8 hours longer than P-NS and 5 hours longer than P-NSF4WD. This is an indication that NSF4 functionalized at a higher rate than NSF4WD.

Some characteristic peaks of the hydration kinetics of Portland cement are highlighted in Fig. 4. Peak A refers to the beginning of hydration. Peak B may represent the formation of C–S–H due to the hydration of C3S, while peak C may denote the renewed formation of ettringite [31,43]. These last two peaks are greater for the pastes with the addition of NS and NSF, being later and less intense for the paste with NS functionalized in the presence of dichloromethane. Therefore, it is clear that functionalization can interfere with hydration reactions. Both functionalizing processes presented delayed reactions and less accumulated heat release than P-NS and P-REF, increasing the time needed to reach the maximum heat value. These results are expected, since the use of these materials is characterized by providing an initial delay in hydration, on the other hand, the reactions are more intense and complete over time, improving the degree of hydration of cementitious materials [6,10,31- 33,36]. In the P-NSF4 paste, with NS functionalized by the traditional method, a greater extension of the dormancy period is observed, marked by a greater initial delay.

3.2.2. Compressive resistance

The results obtained for the compressive resistance of all mortars analyzed at ages of 1, 3, 7 and 28 days can be seen in Figure 5. Note the systematic increase in the resistance values of mortars with NS, NSF4 and NSF4WD in relation to the reference, from the initial measurement ages.

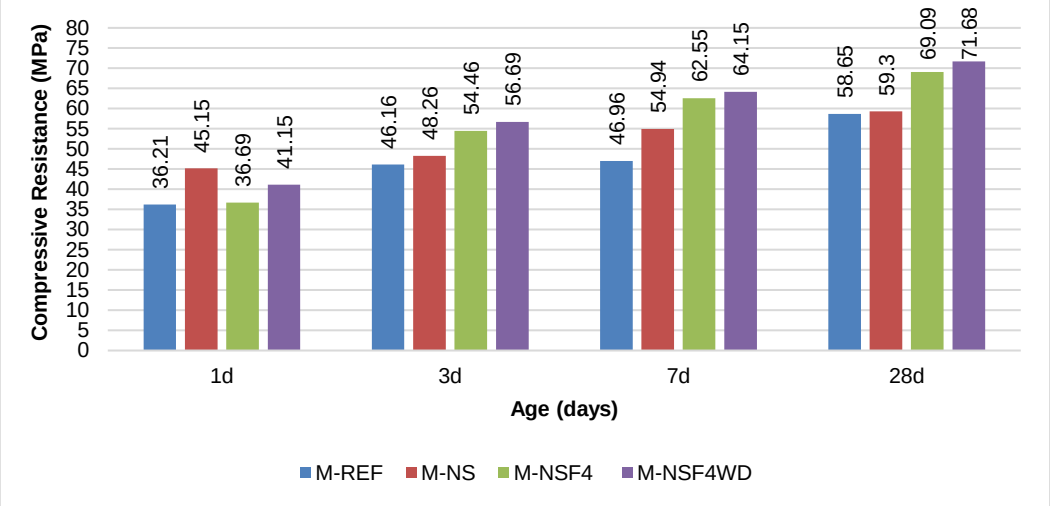

Figure 5. Result of the compressive resistance of mortars at ages of 1, 3, 7 and 28 days.

The M-NS mortar was the one with the highest resistance after 1 day of hydration (44.15 MPa), a value 25% higher than the M-REF. This result is expected and already reported in the literature [7-11,21,28,38,45,47], which attributes this behavior to the high surface area of the NS, functioning as nucleation points that increase the reaction rate and quantity of hydration products formed at this age, as observed in the calorimetry results. It can be seen that this increase was smaller for the M-NSF4 and M-NSF4WD mortars, 2% and 14% respectively, due to the treatment of the NS surface with amine groups, which causes a poisoning effect on the nucleation sites by releasing ions which prevent the growth of hydrates in this location, mitigating the accelerating effect characteristic of NS [1,2,36].

For all ages analyzed, the samples with NS and NSF presented compressive resistance higher than the reference, however, as hydration progresses, the resistance gain of M-NS tends to decrease, unlike the values of M-NSF4 and M- NSF4WD. After 3 days of hydration, it is possible to observe that M-

NSF4WD presents not only the greatest gain in relation to REF but also the highest resistance value observed among all specimens (23% and 56.69 MPa), followed by M-NSF4 (18% and 54.46 MPa) and M-NS (4.5% and 48.26 MPa). The benefit of functionalization is greater as hydration progresses, especially after 7 days. At 28 days, both mortars with NSF have greater resistance than M-REF, with gains greater than 17%, while M-NS presented a value similar to the reference. The reduction in the resistance gain of the mortar with NS occurs due to the initial acceleration of the hydration reactions that quickly form a layer of CSH on the surface of the material, hindering the progression of cement hydration by blocking the diffusion of ions through the hydrates [31, 32, 36].

In order to check if the results found were significant, analysis of variance was performed at 1, 3, 7 and 28 days, the main age of evaluation, as shown in Table 5. The p-value obtained through analysis of variance for all the analyzes carried out were lower than the 0.05 significance level. Therefore, it is possible to state that there is a significant difference in the mechanical performance of the mortars.

Table 5. Analysis of variance of mortar compressive strength results

Days	*SQ*	*MQ*	*F*	*P-value*	*Result*
1 day	168.5929	56.1976	33.8859	0.0000676	**Significant**
3 days	176.0507	58.6835	14.3104	0.0014005	**Significant**
7 days	389.0558	129.6852	36.3725	0.0000520	**Significant**
28 days	697.8316	232.6105	66.5308	0.0000051	**Significant**
SQ = Sum of squares; MQ = Mean of squares; F= Fisher parameter for the significance test; p-value= probability of significance.					

To find out which mortars resulted in greater or lesser mechanical performance, the Duncan test was done. The results are presented in Table 6.

Table 6: Statistical analysis (Duncan test) of the compressive strength of mortars

Days	Mortar	Medium compressive strength	Standard deviation	Group 01	Group 02	Group 03
1 day	M-REF	36.69	0.94	X		
	M-NS	45.16	1.63		X	
	M-NSF4	36.69	1.26	X		
	M-NSF4WD	42.85	1.22		X	
3 days	M-REF	48.02	1.07	X		
	M-NS	48.26	2.29	X		
	M-NSF4	54.62	1.73		X	
	M-NSF4WD	56.69	2.65		X	
7 days	M-REF	49.94	3.12	X		
	M-NS	55.83	1.64		X	
	M-NSF4	62.73	0.21			X
	M-NSF4WD	64.15	1.33			X
28 days	M-REF	58.65	2.75	X		
	M-NS	59.30	2.06	X		
	M-NSF4	69.09	0.09		X	
	M-NSF4WD	71.68	2.5		X	

On the 1st day of hydration, it is observed that the resistance value of the M-NSF4 mortar is closer to the M-REF, corroborating with the results obtained from isothermal conduction calorimetry, in which it was possible to conclude that, when compared to NS and NSF4WD, the inclusion of NSF4 delays the release of heat, resulting in a lower resistance value at this age. From the 3rd day, P-NSF4 obtains a significant gain in resistance due to the intense pozzolanic reaction that occurs after the initial delay, approaching M-NSF4WD. Already after 7 days, 3 groups of resistance with different behaviors form: (1) the M-REF mortar tends to stabilize the resistance value and has the lowest magnitude among the samples analyzed, (2) the M-NS returns to gain strength with an intensity greater than M-REF, but still far from the mortars (3) M-NSF4 and M-NSF4WD, which have the highest values observed.

Finally, after 28 days of hydration, 2 groups with very characteristic resistances are formed. Group 1 (M-REF and M-NS) has the lowest resistance and group 2 (M-NSF4 and M-NSFWD) has the highest resistance. It is possible to see that the mortars with NSF presented statistically equal resistances with an increasing tendency in relation to both the M-REF and M-NS samples. Therefore, application of functionalized NS without dichloromethane in cementitious composites is as efficient as using the traditional method, since there was no

3.2.3. Porosity

Table 7 presents the data obtained using mercury intrusion porosimetry (MIP), allowing to evaluate information related to total porosity, average pore diameter, reduction in pore size and porosity in the 50-10nm size range.

Table 7: Result of paste porosimetry at the age of 28 days

Folder	Porosity total (%)	Average pore diameter (nm)	Relative reduction in average pore size (%)	Volume of intruded mercury (mL/g)	
				Medium capillary (50-10nm)	
				(mL/g)	(%) in relation to REF
P-REF	12.7	20.1	-	1,776	100%
P-NS	11.7	14.3	29	1,639	92%
P-NSF4	11.4	15.3	24	1,646	93%
P-NSF4WD	12.2	18.2	10	1,442	81%

Initially, it can be seen that P-REF presented porosity (12.75%) greater than all other pastes with nanosilica. The refinement in the porous structure can be attributed to both the high reactivity and the pozzolanic activity of NS, which densifies the microstructure of the materials by consuming CH from Portland cement hydration reactions to form an additional amount of C–S–H. Furthermore, with functionalization, NS can still be available at the end of setting when the main C–S–H part of the cement paste is already formed. Therefore, it is possible for NSF to penetrate the nanopores of the C–S–H group network and fill them without reacting or forming even more C–S–H between the sheets, joining them or not, reducing the voids in the material [4 ,7,8,32,30-33,46]. This reduction is greatest in P-NSF4 (11.4 nm), followed by P-NS (11.69 nm) and P-NSF4WD (12.23 nm).

The addition of NS and NSF also allowed a reduction in the average pore size observed in the pastes. The greatest reduction was observed for P-NS (29%), followed by P-NSF4 (24%). It is worth mentioning that, in relation to the reference, the P-NSF4WD paste presents a slightly lower reduction in pore diameter (10%), however this behavior is followed by lower porosity in the size range of 50-10 nm (19%) between all samples. It is important to highlight that reducing the volume of micropores influences the durability of cementitious materials, as they account for the permeability of the matrix and the absorption of aggressive agents [50].

IV. CONCLUSIONS

This article sought to investigate the viability of excluding dichloromethane from the traditional NS functionalization process, through the development of an alternative process, leaner in its steps and materials used. Verification of the process efficiency occurred in two stages: Characterization of the functionalized material and characterization of cementitious composites with the addition of NSF.

The characterization of NSF4 and NSF4WD allowed us to prove that both functionalizations were successful in grafting APTES onto the surface of the NS. NSF4WD showed stability in aqueous solution close to NSF4, proven by the Zeta potential result. The results obtained from DLS, XRD, FTIR and TGA indicated a higher APTES content in the traditional process, possibly referring to the greater saturation of the coupling agent on the NSF4 surface. Although the amount of APTES functionalized in NSF4 was slightly higher, NSF4WD also showed adequate and efficient functionalization.

The analysis of cementitious composites showed that the application of the two different types of NSF provided satisfactory results. The pastes with functionalized materials showed characteristic heat release kinetics, delaying the initial reactions, the most prominent characteristic of P-NSF4, and showing similar behavior after 60 hours of hydration. The compressive strength values obtained from the mortars at 28 days were higher than those of the reference material and pure NS. Despite the higher APTES content present in NSF4, the statistical analysis showed that the resistance values of mortars with NSF are statistically similar and show an increasing trend in relation to REF and NS. As for porosity, NSF's enabled a reduction in both pore size and total porosity when compared to the reference paste.

In summary, this research clearly demonstrates the potential of direct functionalization of NS with 3-Aminopropyltriethoxysilane (APTES), without the use of a chemical solvent. The alternative NSF4WD production process proved to be effective in grafting APTES onto the NS surface, as it presented results similar to the traditional process, in addition to being adequate and compatible with the literature. Furthermore, the alternative functionalization procedure complies with Green Chemistry principles, not using toxic solvents and minimizing negative impacts on the environment, reducing the amount of reagents and the number of steps in the process, as it incorporates the reagents into the final product. Even so, the mechanics of the NS/APTES interaction are not fully understood, requiring more specific research that seeks to understand this interaction and explore new applications of NSF for the cement industry.

ACKNOWLEDGEMENTS

The authors are grateful to the National Council for Scientific and Technological Development (CNPq), the National Council for the Improvement of Higher Education (CAPES), Federal District Research Support Foundation (FAPDF) and the Ibero-American Science and Technology for Development Program (CYTED) for financial support for conducting research in the Program of Post-graduation in Structures and Civil Construction of the University of Brasília (PECC/UnB).

REFERENCES

[1]. Luana SG, Antônia CRF, Marcos CS (2018) About silica and its particularities. Revista Virtual de Química. https://rvq.sbq.org.br/pdf/v10n4a19

[2]. Juliana SV, Yuri SB, Joao HSR et al (2023) Hydration, mechanical performance and porosity of Portland cement pastes with functionalized nanosilica with APTES. Developments in the Built Environment. https://doi.org/10.1016/j.dibe.2023.100157

[3]. Yonathan R (2018) Nanoparticles as concrete additives: Review and perspectives. Construction and Building Materials. https://doi.org/10.1016/j.conbuildmat.2018.04.214

[4]. Renan RR, Matheus ICS, Joao HSR, Rodrigo ML (2022) Innovative lowcost system for early age E-modulus monitoring of cement pastes: validation and application to nanosilica-added and limestone-calcined clay cements. Materials and Structures. https://doi.org/10.1617/s11527-021-01849-w

[5]. Chunrong R, Li H, Jun L, Zhongyuan L, Yunhui N (2020) Preparation and properties of nanosilica-doped polycarboxylate superplasticizer. Construction and Building Materials. https://doi.org/10.1016/j.conbuildmat.2020.119037.

[6]. Giovana C, Philippe J, Paulo J.M (2014) Exploring the potential of siloxane surface modified nano-SiO2 to improve the Portland cement pastes hydration properties. Construction and Building Materials. https://doi.org/10.1016/j.conbuildmat.2013.12.028.

[7]. Andréia P, Yuri FSB, João HSR, Maria JS (2023) Effects of functionalized nanosilica with low aminosilane content on the mechanical properties and microstructure of cementitious materials. International Journal of Advances in Engineering and Technology. https://10.5281/zenodo.8330421.

[8]. Gu, Y et al (2016) Synthesis of nanoSiO2@PCE core-shell nanoparticles and its effect on cement hydration at early age. Construction and Building Materials. http://dx.doi.org/10.1016/j.conbuildmat.2016.03.093.

[9]. Gu Y et al (2018) Effects and mechanisms of surface-treatment of cementitious materials with nanoSiO2@PCE core-shell nanoparticles. Construction and Building Materials. https://doi.org/10.1016/j.conbuildmat.2018.01.082.

[10]. Yuri F, Martins B, Gabriel O, João R (2021) Influence of functionalized nanosilica with different functional groups in the properties of cementitious composites: A review. Research, Society and Development. http://dx.doi.org/10.33448/rsd-v10i8.17349.

[11]. Juliana V, Gabriel M, Almeida O, João R (2020) Effect of amine functionalized nanosilica on the cement hydration and on the physicalmechanical properties of Portland cement pastes. Journal of Nanoparticle Research.

[12]. Lourenço S (2010) Functionalized silica particles containing TR3+ complexes for application as markers in biological assays. Doctoral Thesis in in Chemistry, Publication E.DM-XX/23, Department of in Chemistry, University of São Paulo, São Paulo, SP, 192p.

[13]. Gabriel O, Yuri F Juliana V, Rêgo, João R (2020) Synthesis and characterization of functionalized nanosilica for cementitious composites: review. Journal of Nanoparticle Research

[14]. Agência Internacional de Pesquisa em Câncer (IARC), https://www.iarc.who.int/.

[15]. Vidal S (2020) Safety First: A Recent Case of a Dichloromethane Injection Injury, ACS Central Science

[16]. Lenardão J, Freitas A, Dabdoub J, Batista F, Silveira C (2003) Green chemistry: the 12 principles of green chemistry and it insertion in the teach and research activities Quim. https://doi.org/10.1590/S0100-40422003000100020.

[17]. Serafim S, Bessler E, Lemos S, Sales A, Ellena, J (2007) The preparation of new oxoniobium(V) complexes from hydrated Niobium(V) Oxide: the crystal and molecular structure of Oxotris(2-pyridinolato-N-oxide)niobium(V). Transition Metal Chemistry. https://doi.org/10.1007/s11243-006-0142-x

[18]. Yuri F, João R, Valdirene C, Daniel A (2020) Ultrasonication effect of silica fume and colloidal nanosilica on cement pastes. Revista Matéria. https://doi.org/10.1590/S1517-707620200004.1147.

[19]. Pan F et al (2020) The significance of dispersion of nano-SiO2 on early age hydration of cement pastes. Materials and Design. https://doi.org/10.1016/j.matdes.2019.108320.

[20]. Xia L, Pengkun H, Heng C (2021) Effects of nanosilica on the hydration and hardening properties of slag cement. Construction and Building Materials. https://doi.org/10.1016/j.conbuildmat.2021.122705.

[21]. Liu X, Pan F, Shu X, Ran Q (2020) Effects of highly dispersed nano-SiO2 on the microstructure development of cement pastes. Materials and Structures/Materiaux et Constructions.

[22]. Yogiraj S, Kejin W (2021) Influence of dispersants and dispersion on properties of nanosilica modified cement-based materials. Cement and Concrete Composites. https://doi.org/10.1016/j.cemconcomp.2021.103969.

[23]. Chunlong H et al (2020) Potential Effect of Surface Modified Nano-SiO2 with PDDA on the Cement Paste Early Hydration. ChemistrySelect.

[24]. Sun, J, Shi H, Qian B, Xu Z, Li W, Shen X (2017) Effects of synthetic C-S-H/PCE nanocomposites on early cement hydration. Construction and Building Materials.

[25]. ABNT - Brazilian Association of Technical Standards. NBR 16606: Portland Cement - Determination of normal consistency paste. Rio de Janeiro, 2018.

[26]. ABNT - Brazilian Association of Technical Standards. NBR 16697: Portland Cement - Requirements. Rio de Janeiro, 2018.

[27]. ABNT - Brazilian Association of Technical Standards. NBR 7215: Portland Cement - Determination of compressive strength of cylindrical specimens. Rio de Janeiro, 2006.

[28]. Ordóñez L (2013) Mitigation of autogenous shrinkage in high strength microconcrete with addition of superabsorbent polymers and shrinkage reducing additive. 160 f. Dissertation (Master in Structures and Civil Construction) - University of Brasília, Brasília, 2013.

[29]. João R, Rojas M, Terrades M, Fernandez L, Morales R, Rojas S (2019) Effect of partial substitution of highly reactive mineral additions by nanosilica in cement pastes. J. Mater. Civ. Eng.

[30]. Vasconcellos, J.S. (2021). Microstructure of Portland cement pastes with the Incorporation of Functionalized Nanosilica with Amine Groups. Doctoral Thesis in Structures and Civil Construction, Publication E.TD – 08A/21, Department of Civil and Environmental Engineering, University of Brasília, Brasília, DF, 248p.

[31]. Martins, G.L.O. (2022). Microstructure of Portland cement pastes containing functionalized nanosilica with different proportions of aminosilane. Doctoral Thesis in Structures and Civil Construction, Publication E.DM-XXA/22, Department of Civil and Environmental Engineering, University of Brasília, Brasília, DF, 189p.

[32]. Y. S. B. (2023) Effect of functionalization of nanosilica with different ratios shrinkage reducing additive mass in cementitious composites. Doctoral Thesis in Structures and Civil Construction, Publication E.DM-XX/23, Department of Civil and Environmental Engineering, University of Brasília, Brasília, DF, 164p.

[33]. Kang S, Hong S, Choe C, Park M, Rim S, Kimb J (2001) Preparation and characterization of epoxy composites filled with functionalized nanosilica particles obtained via sol-gel process, Polymer. http://dx.doi.org/10.21577/1984-6835.20230070.

[34]. Zhao J, Wang C, Wanga S, Zhang L, Zhang B (2019) Augmenting the adsorption parameters of palladium onto pyromellitic acid-functionalized nanosilicas from aqueous solution, Colloids and Surfaces. https://doi.org/10.1016/j.colsurfa.2019.123581.

[35]. Collodetti G, Gleize P, Monteiro P (2014) Exploring the potential of siloxane surface modified nano-SiO2 to improve the Portland cement pastes hydration properties, Construction and Building Materials. https://doi.org/10.1016/j.conbuildmat.2013.12.028.

[36]. Katiyar A, Nandi T, Katiyar P, Dhar P, Prasada N (2019) Enhanced cluster order–disorder transitioninduced dilatancy in silane-functional nanosilica colloids, The Royal Society of CChemistry https://doi.org/ 10.1039/c8sm02406e.

[37]. Suh H, Kim G, Cho S, Li P, Son D, Koo D, Lim J, Cho C (2023) Comparative analysis of the synergistic effects of hybrid nanomaterial reinforcement in cementitious composites: A perspective for pore refinement and thermal resistance. Construction and Building Materials. https://doi.org/10.1016/j.conbuildmat.2023.132856.

[38]. Moreno Y, Cardoso M, Marco F, Moncada S, Santos J (2016) Effect of SiCl4 on the preparation of functionalized mixed-structure silica from monodisperse sol–gel silica nanoparticles. Chemical Engineering Journal. https://doi.org/10.1016/j.cej.2016.02.027.

[39]. Yan C, Fan X, Li J, Shen S (2011) Study of Surface-Functionalized Nano SiO2/Polybenzoxazine Composites, Journal of Applied Polymer Science. https://doi.org/10.1002/app.33383.

[40]. Dintcheva N, Arrigo R, Gambarotti C, Carroccio S, Coiai S, Filippone G (2015) Advanced ultra-high molecular weight polyethylene/antioxidant-functionalized carbon nanotubes nanocomposites with improved thermo-oxidative resistance. Journal of Applied Polymer Science. https://doi.org/10.1002/APP.42420.

[41]. Hussain S, Zhao Z, Yong Y, Zhang C (2023) Effect of SiO2 surface modification on the filler-reinforced interfaces in SiO2-filled functional styrene butadiene rubber composites, Journal of Applied Polymer Science. https://doi.org/10.1002/app.54401.

[42]. Li Y, Li H, Jin C, Wang Z, Hao J, Li Y, Liu J (2021) Multi-scale investigation and mechanism analysis on Young's modulus of C-S-H modified by multi-walled carbon nanotubes. Construction and Building Materials. https://doi.org/10.1016/j.conbuildmat.2021.125079.

[43]. Moghbeli MR, Khajeh A, Alikhani M (2017) Nanosilica reinforced ion-exchange polyHIPE type membrane for removal of nickel ions: Preparation, characterization and adsorption studies. Chemical Engineering Journal. http://dx.doi.org/10.1016/j.cej.2016.10.048.

[44]. Fang Y, Wang J, Ma H, Wang L, Qian X, Qiao P (2021) Performance enhancement of silica fume blended mortars using bio-functionalized nano-silica. Construction and Building Materials. https://doi.org/10.1016/j.conbuildmat.2021.125467.

[45]. Ren C, Hou L, Li J, Lu S, Niu Y (2020) Preparation and properties of nanosilica-doped polycarboxylate superplasticizer. Construction and Building Materials. https://doi.org/10.1016/j.conbuildmat.2020.119037.

[46]. Gyeongryul K, Suh H, Cho S, Nezhad S, Seok S, Choi C, Bae S (2022) Synergistic strengthening mechanism of Portland cement paste reinforced by a triple hybrid of graphene oxide, functionalized carbon nanotube, and nano-silica. Construction and Building Materials. https://doi.org/10.1016/j.conbuildmat.2022.129017.

[47]. Branda F, Silvestri B, Luciani G, Costantini A, Tescione F (2010) Synthesis structure and stability of amino functionalized PEGylated silica nanoparticles. Construction and Building Materials. https://doi.org/10.1016/j.colsurfa.2010.05.036.

[48]. Lourenço AVS (2010) Functiomalized silica particles's containing TR3+ complees for application as markers in biological assays. Doctoral Thesis.

[49]. Mehta PK, Monteiro PJM (2014) Concrete: Structure, properties and materials, Ibracon.

[50]. Khosroshahi M, Tehrani I, Nouri A Fabrication and characterization of multilayer msio2@fe3o4@au mesoporous nanocomposite for near-infrared biomedical applications, AdvNanoBioM&D.